Dynamic Characteristics of Vibratory Gyro-accelerometer

Payal Verma, Ram Gopal
MEMS & Microsensors Group
CSIR-CEERI, Pilani
Rajasthan, India
payalsedha@gmail.com, ram@ceeri.ernet.in

Sandeep Kumar Arya
Department of Electronics & Communication
GJUS&T, Hisar
Haryana, India
arya1sandeep@gmail.com

***Abstract*— This paper presents a systematic approach in reaching governing equation for microgyroaccelerometer. The study is focused on to analyze the dynamic characteristics of vibratory microgyroaccelerometer. In this device, the mechanical structure is excited into oscillatory motion. The angular velocity input to the sensor is then multiplied by the periodic driven motion. A demodulation is required to recover the angular velocity input and linear acceleration from the sense responses, as the governing differential equations for the Gyro-accelerometer input and output are time variant. The frequency responses for the time variant linear system is obtained through the demodulation and low pass filtered steady-state output to sinusoidal excitation. The frequency response, thus, obtained are validated with MATLAB Simulink data.**

Keywords- Gyro-accelerometer, MEMS

I. INTRODUCTION

In the current technological scenario, MEMS technology has emerged as one of the most promising technologies. Advancements in micro-electromechanical system (MEMS) technologies have led to the development of miniaturized accelerometers and gyroscopes. Most of the micromachined gyroscopes are based on the concept of Coriolis force being generated and sensed by the mechanical part [1]. The concept of utilizing the vibrating elements to induce and detect Coriolis force involving no rotating parts (requiring bearings) has proven to be very effective. There has been significant progress in the past couple of years, meeting the requirements of several applications such as navigation especially in automotive, aerospace and military applications. These microgyros can be used in conjunction with micromachined accelerometers to provide heading information for inertial navigation purposes. There is an enormous demand for the development of a single inertial system that can measure both linear acceleration and angular rate. However very little efforts have been put in this direction due to the complexities involved [2-5].

In the case of multi-axis sensors, it is easy to design the signal processing circuit because of its nearly identical setup for each axis. However, since the operating frequencies in the multi-axis sensors are in the same frequency region, they have large cross-axis sensitivities which are an undesirable feature for inertial sensors. In this regard, the gyro-accelerometer multi-measurement system has better capability of reducing the cross-axis sensitivity as it has different operating frequencies for a gyro and acceleration actions.

Vibratory rate Gyro-accelerometer consists of a two DOF structure that can oscillate in orthogonal directions on a plane and transfer inertial energy from drive mode to sense mode when the Coriolis effect is induced.

In this paper, the structural model of Gyro-accelerometer with the demodulation and filtering processes is studied to investigate the frequency response. Using harmonic angular rate as input [6], the response of the sensor after demodulation and filtering is calculated.

II. GYRO-ACCELEROMETER DYNAMICS

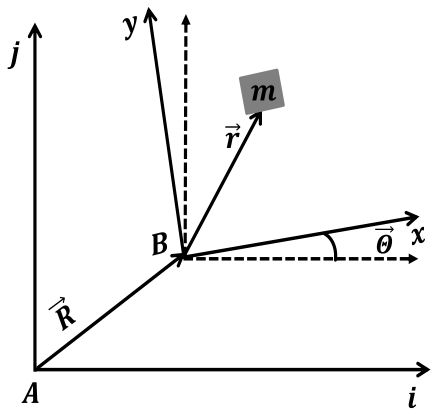

Figure 1. Time derivative of a vector in a non-inertial frame.

Accelerations for the gyroscope [7, 8] are obtained using a non-inertial coordinate frame of reference. Linear acceleration term in the case of gyro-accelerometer is retained by using the same. Mass, m can be assumed to be a rigid body shown in Fig.1, with a positive vector $\vec{r}_B$ in reference to the rotating frame of reference **B**. The position and orientation of the frame of reference **B** in reference to the inertial frame of reference **A** are $\vec{R}$ and $\vec{\Theta}$ respectively. Therefore, position of proof mass with respect to inertial frame of reference is,

$$\vec{r}_A = \vec{R} + \vec{r}_B \quad (1)$$

Now considering the rotation angle vector $\vec{\Theta}$ of the system with reference to non-inertial frame of reference and assuming it along with other position vectors time dependent, the double time derivative of (1) is written as,

$$\ddot{\vec{r}}_A = \ddot{\vec{R}} + \ddot{\vec{r}}_B + 2(\dot{\vec{\Theta}} \times \dot{\vec{r}}_B) + \dot{\vec{\Theta}} \times \left(\dot{\vec{\Theta}} \times \vec{r}_B\right) + \ddot{\vec{\Theta}} \times \vec{r}_B$$

Assuming that the non-inertial frame **B** of Gyro action rotates with angular velocity $\vec{\Omega}$, the equation of motion of Gyro-accelerometer can be written as (using Newton's second law of motion) ,

$$\boldsymbol{F} = m\left[\ddot{\vec{R}} + \ddot{\vec{r}} + 2\vec{\Omega} \times \dot{\vec{r}} + \dot{\vec{\Omega}} \times \vec{r} + \vec{\Omega} \times \left(\vec{\Omega} \times \vec{r}\right)\right],$$

Where,

- The first term with in square bracket is the linear acceleration of the Gyro frame with respect to the inertial frame.
- The second term is the linear acceleration of the mass in the Gyro frame.
- The third term is the Coriolis acceleration, which appears only if the equations of the motion are written in non-inertial frame.
- The fourth and fifth terms represent Euler's accelerations and centrifugal accelerations.

Considering linear acceleration and decomposing the motion into two principle oscillation directions , the drive and sense directions, the respective two equations of motion can be expressed as,

$$m\ddot{x} + c_x\dot{x} + k_x x = 2m\dot{y}\Omega_z + my\dot{\Omega}_z + mx\Omega_z^2 - ma_x\cos\theta - ma_y\sin\theta + F_d(t)\,, \quad (2)$$

$$m\ddot{y} + c_y\dot{y} + k_y y = -2m\dot{x}\Omega_z - mx\dot{\Omega}_z + my\Omega_z^2 + ma_x\sin\theta - ma_y\cos\theta\,. \quad (3)$$

The mass m is electrically driven by force $F_d(t)$. All the forces other than $F_d(t)$, such as centrifugal force, Euler's force and forces due to external accelerations a_x and a_y, are neglected as $F_d(t)$ is comparatively higher than these forces. Angular rates are much smaller than the driving frequency, therefore the terms $y\dot{\Omega}_z\,, \dot{y}\Omega_z, x\Omega_z^2$ and $y\Omega_z^2$ can be neglected, resulting in the simplified 2-DOF equations of motion:

$$\ddot{x} + 2\lambda_x\dot{x} + \omega_x^2 x = \frac{F_d(t)}{m}\,, \quad (4)$$

$$\ddot{y} + 2\lambda_y\dot{y} + \omega_y^2 y = -2\dot{x}\Omega_z - x\dot{\Omega}_z + a_x\sin\theta - a_y\cos\theta\,. \quad (5)$$

Where,

$$\omega_x^2 = \omega_y^2 = \frac{k_x}{m} = \frac{k_y}{m};\ \lambda_x = \lambda_y = \frac{c_x}{2m} = \frac{c_y}{2m}.$$

The single mass 2-DOF dynamical system has two independent resonant frequencies, drive resonant frequency and sense resonant frequency denoted by ω_x and ω_y respectively. In order to have enhanced performance, both the modes must match. This can be achieved by adjusting k_x and k_y equivalent to each other. However fabrication imperfections and other factors such as temperature changes may result in a drift in the driven mode [9]. It is therefore suggested to use a closed–loop control system to ensure that the driven mode is excited at its resonance frequency.

III. Steady State Response

The settled solution of sense is comprised of both gyro as well as acceleration actions. In order to differentiate both of these actions, the analysis of sense amplitude is vital to distinguish the different frequency ranges within which their respective effects are separately dominant. Hence, we can assume, $F_d(t) = F_o\sin(\omega t)$.

The settled transient solution of equation (4) is

$$x(t) = f_o\mathcal{A}_x(\omega)\sin(\omega t + \phi_x(\omega))$$

Where,

$$\mathcal{A}_x(\omega) = \frac{1}{\sqrt{(\omega_x^2 - \omega^2)^2 + 4\lambda_x^2\omega^2}},$$

$$\phi_x(\omega) = -\tan^{-1}\frac{2\lambda_x\omega}{\omega_x^2 - \omega^2}\ ;\ f_o = \frac{F_o}{m}.$$

Considering the harmonic angular rate, their frequency is small compared to operation frequency,

$$\Omega_z = \Omega_o\cos(\alpha t).$$

Therefore the settled solution of for (5) is written as

$$y(t) = A_1\cos\{(\omega+\alpha)t + \phi_x(\omega) + \phi_y(\omega+\alpha)\} + A_2\cos\{(\omega-\alpha)t + \phi_x(\omega) + \phi_y(\omega-\alpha)\} + \mathcal{R}_{ex}\mathcal{A}_y(\omega)\sin\left(\omega t + \phi_y(\omega)\right). \quad (6)$$

Where,

$$A_{1,2} = -\Omega_o f_o\mathcal{A}_x(\omega)\left(\omega \pm \frac{1}{2}\alpha\right)\mathcal{A}_y(\omega \pm \alpha),$$

$$\mathcal{A}_y(\omega) = \frac{1}{\sqrt{\left(\omega_y^2 - \omega^2\right)^2 + 4\lambda_y^2\omega^2}},$$

$$\phi_y(\omega) = -\tan^{-1}\frac{2\lambda_y\omega}{\omega_y^2 - \omega^2}\,, \quad (7)$$

Since the input is modulated by sinusoidal function, its output must be demodulated, we define demodulated signals

$y_p(t) = y(t)\cos(\omega t)$ and $y_q(t) = y(t)\sin(\omega t)$, in-phase and quadrature signal respectively. The corresponding solution of (6) after using trigonometric identities are represented by,

$$y_p(t) = \overline{A}\{\cos(2\omega t + \phi_x(\omega) + \overline{\phi}) + \cos(\phi_x(\omega) + \overline{\phi})\} \times \cos(\alpha t + \Delta\phi) - \delta A\{\sin(\phi_x(\omega) + \overline{\phi}) + \sin(2\omega t + \phi_x(\omega) + \overline{\phi})\}\sin(\alpha t + \Delta\phi) + \tfrac{1}{2}\mathcal{R}_{ex}\mathcal{A}_y(\omega)\left\{\sin\phi_y(\omega) + \sin\left(2\omega t + \phi_y(\omega)\right)\right\}, \quad (8)$$

$$y_q(t) = \overline{A}\{\sin(2\omega t + \phi_x(\omega) + \overline{\phi}) - \sin(\phi_x(\omega) + \overline{\phi})\} \times \cos(\alpha t + \Delta\phi) - \delta A\{\cos(\phi_x(\omega) + \overline{\phi}) - \cos(2\omega t + \phi_x(\omega) + \overline{\phi})\}\sin(\alpha t + \Delta\phi) + \tfrac{1}{2}\mathcal{R}_{ex}\mathcal{A}_y(\omega)\left\{\cos\phi_y(\omega) - \cos\left(2\omega t + \phi_y(\omega)\right)\right\}, \quad (9)$$

The modified parameters included in (8) and (9) are defined as,

$$\bar{A} = \frac{1}{2}(A_1 + A_2),$$

$$\delta A = \frac{1}{2}(A_1 - A_2),$$

$$\bar{\phi} = \frac{1}{2}\left[\phi_y(\omega + \alpha) + \phi_y(\omega - \alpha)\right],$$

and,

$$\Delta\phi = \frac{1}{2}\left[\phi_y(\omega + \alpha) - \phi_y(\omega - \alpha)\right].$$

The terms $\cos(\alpha t + \Delta\phi)$ and $\sin(\alpha t + \Delta\phi)$ in (8) and (9) are the output signals, related to the angular rate leading by phase shift, $\Delta\phi$, which is distorted due to frequency, α. Other terms have doubled frequency and those must be removed by low-pass-filtering after demodulations.

After filtration (8) and (9) are given by,

$$y_{lp}(t) = \overline{A}\cos(\phi_x(\omega) + \overline{\phi})\cos(\alpha t + \Delta\phi) - \delta A\sin(\phi_x(\omega) + \overline{\phi})\sin(\alpha t + \Delta\phi) + \tfrac{1}{2}\mathcal{R}_{ex}\mathcal{A}_y(\omega)\sin(\phi_y(\omega)) \quad (10)$$

$$y_{lq}(t) = -\overline{A}\sin(\phi_x(\omega) + \overline{\phi})\cos(\alpha t + \Delta\phi) - \delta A\cos(\phi_x(\omega) + \overline{\phi})\sin(\alpha t + \Delta\phi) + \tfrac{1}{2}\mathcal{R}_{ex}\mathcal{A}_y(\omega)\cos(\phi_y(\omega)) \quad (11)$$

Equations (10) and (11) represent low-pass-filtered in-phase and quadrature components of sensor outputs to the sinusoidal input; that includes both angular rate signal and acceleration. Rewriting the equations, using trigonometric identities, we have,

$$y_{lp}(t) = A_p\cos(\alpha t + \psi_p) + \frac{1}{2}\mathcal{R}_{ex}\mathcal{A}_y(\omega)\sin\left(\phi_y(\omega)\right), \quad (12)$$

$$y_{lq}(t) = A_q\cos(\alpha t + \psi_q) + \frac{1}{2}\mathcal{R}_{ex}\mathcal{A}_y(\omega)\cos\left(\phi_y(\omega)\right). \quad (13)$$

Where,

$$A_p^2 = \overline{A}^2\cos^2(\phi_x(\omega) + \overline{\phi}) + \delta A^2\sin^2(\phi_x(\omega) + \overline{\phi}),$$

$$A_q^2 = \overline{A}^2\sin^2(\phi_x(\omega) + \overline{\phi}) + \delta A^2\cos^2(\phi_x(\omega) + \overline{\phi}),$$

$$\psi_p = \Delta\phi + \Delta\varphi_p,$$

$$\psi_q = \Delta\phi + \Delta\varphi_q,$$

$$\Delta\varphi_p = \tan^{-1}\left[\frac{\delta A}{\overline{A}}\tan(\phi_x(\omega) + \overline{\phi})\right],$$

$$\Delta\varphi_q = -\tan^{-1}\left[\frac{\delta A}{\overline{A}}\cot(\phi_x(\omega) + \overline{\phi})\right].$$

It may be observed that in the first terms of in-phase and quadrature output signals (12) and (13) are distorted both in amplitudes, A_p, and A_q along with respective phases, ψ_p and ψ_q. At the same time, the acceleration term in these equations are unaffected by, α. From these equations, it can be deduced that at the sense frequency, ω_y, $\phi_y(\omega) = -\pi/2$ (see (7)). As a result, both terms are vanished in quadrature equation (13), whereas in in-phase component (12), the sensor output has the contribution of acceleration also along with gyro action. Thus, with the help of sensor output (12) and (13), the angular rate as well as acceleration can be found out. At low frequency range the gyro action is dominated by the acceleration term whereat acceleration terms become frequency independent. Therefore, from low frequency range, acceleration, $\mathcal{R}_{ex}$, can be estimated. Subsequently, by compensating acceleration term in equations (12) and (13), gyro action and thereby angular rate frequency, α, can be obtained.

IV. Results and Discussion

Fig.2 shows the amplitude variation of in-phase, A_p, and quadrature component, A_q , with angular rate frequency, α. At $\omega = \omega_y$, in-phase component is maximum at $\alpha = 0$ and decreases with increase of α, whereas quadrature component is nearly equal to zero. But at $\omega = 0.95\,\omega_y$ and $\omega = 1.05\omega_y$,the amplitude of in-phase and quadrature components are almost same and is maximum at, $\alpha = 0.048\,\omega_y$ for $\omega = 1.05\,\omega_y$, whereas maximum position at $\omega = 0.95\,\omega_y$ shifts towards $\alpha = 0.052\,\omega_y$. At drive frequency $\omega = 1.005\,\omega_y$, the maximum position of amplitude shifts towards $\alpha = .003\omega_y$. Similarly corresponding phase plots also show compensating tendency towards each other. It is thus concluded that the quadrature and in-phase components of gyro-accelerometer can be used for detection of angular velocity and linear acceleration by using compensator.

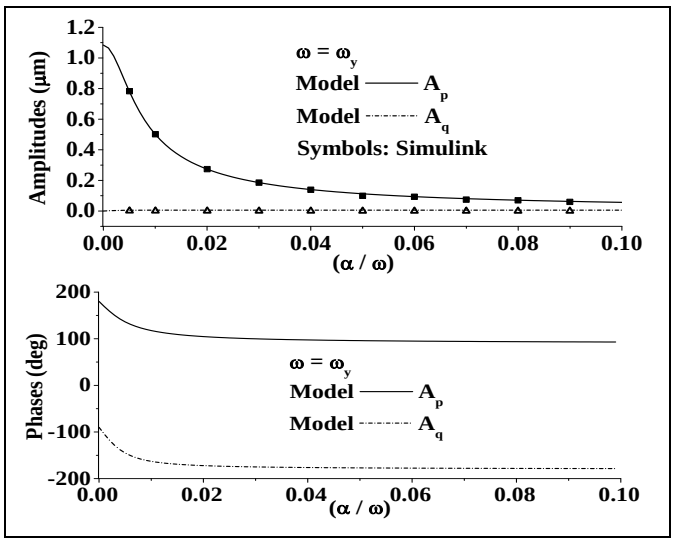

(a)

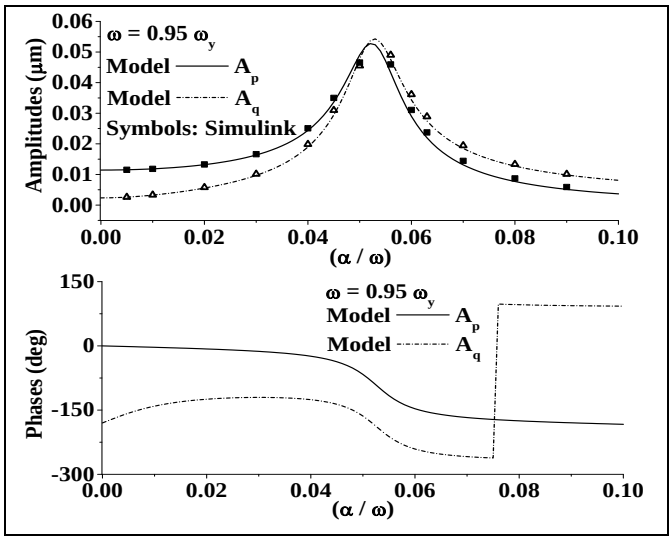

(b)

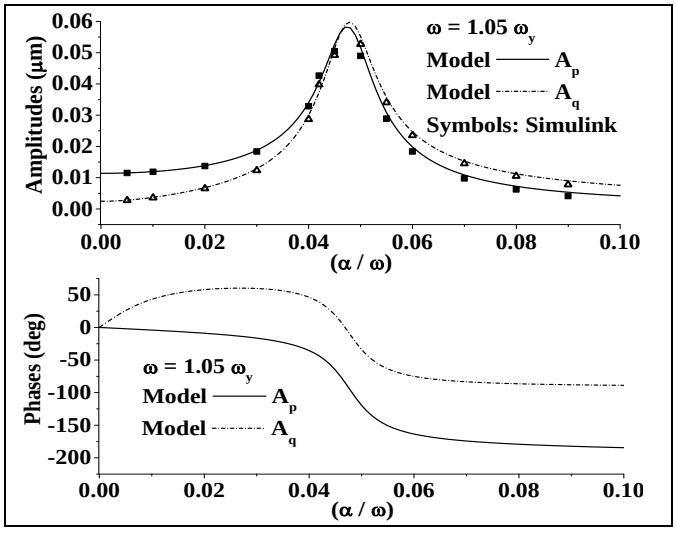

(c)

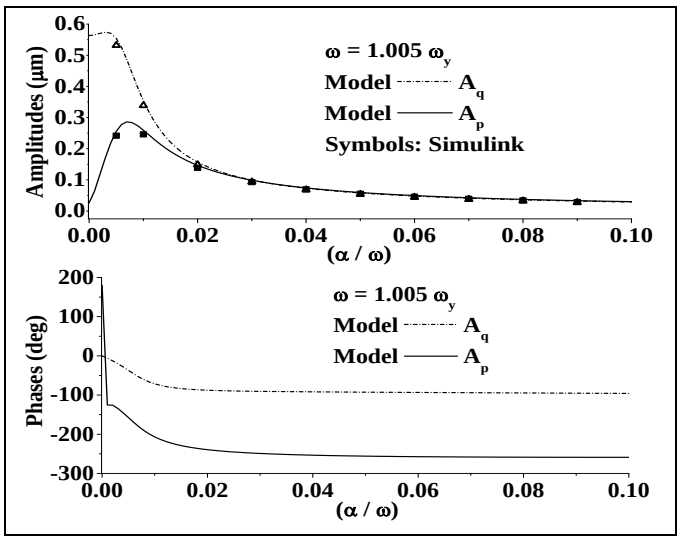

(d)

Figure 2. Frequency response curves: (a) amplitudes and phases at $\omega = \omega_y$, (b) amplitudes and phases at $\omega = 0.95\ \omega_y$, (c) amplitudes and phases at $\omega = 1.05\ \omega_y$, (d) amplitudes and phases at $\omega = 1.005\ \omega_y$, for ($\lambda_x = \lambda_y = 200\ \mathrm{s}^{-1}, F_o = 3.82\mathrm{e}-6\ \mathrm{N}, \Omega_o = 200\ \mathrm{rad\,s}^{-1}, \omega_x = \omega_y = 6.1\ \mathrm{kHz}, \mathrm{m} = 115.01\mathrm{e}-9\ \mathrm{kg}$)

ACKNOWLEDGMENTS

The authors would like to acknowledge Director, CSIR-Central Electronics Engineering Research Institute, Pilani for his valuable guidance. They would like to thank Dr. V.K. Khanna, Head, for their co-operation and support.

REFERENCES

[1] N. Yazdi, F. Ayazi, K. Najafi, "Micromachinedminertial sensors," Proc. IEEE, vol. 86, pp. 1640–1659, 1998.

[2] T. Murakoshi, Y. Endo, K. Fukatsu, S. Nakamura and M. Esashi, "Electrostatically levitated ring-shaped rotational gyro/ accelerometer," Japanese Journal of Applied Physics, vol. 42, pp. 2468-2472, 2003.

[3] J. H. Weng, W. H. Chieng and J. M. Lai, , "Structural design and analysis of micromachined ring-type vibrating sensor of both yaw rate and linear acceleration," Sensors and Actuators A: Physical, vol. 117, no. 2, pp. 230-240, 2005.

[4] R. H. Hulsing, "MEMS inertial rate and acceleration sensor," Proc. IEEE PLANS '98. Pp. 169-176, 1998.

[5] W. T. Sung, T. Kang, J.G. Lee, "Controller design of a MEMS gyro-accelerometer with a single proof mass," International Journal of Control, Automation, and Systems, vol. 6, no. 6, pp.873-882, 2008.

[6] Z. C. Feng, K. Gore, "Dynamic characteristics of vibratory gyroscopes," IEEE Sensors Jpurnal, vol. 4, no. 1, pp. 80-84, 2004.

[7] C. Acar, "Robust micromachined vibratory gyroscopes," Ph.D. dissertation, University of California, Irvine, 2004.

[8] C. Acar, A. Shkel, "MEMS Vibratory Gyroscopes-Structural Approaches to Improve Robustness," Springer, 2009.

[9] Y. Mochida, M. Tamura, K. Ohwada, "A micromachined vibrating rate gyroscope with independent beams for the drive and detection modes," Proc. IEEE Micro-Electro-Mechanical Systems Workshop (MEMS'99), pp. 618-623, 1999.